March 2007

Structure and Polarization in the High T_c Ferroelectric $Bi(Zn,Ti)O_3$-$PbTiO_3$ Solid Solutions

Ilya Grinberg
University of Pennsylvania

Matthew R. Suchomel
University of Pennsylvania

Wotjek Dmowski
University of Tennessee

Sara E. Mason
University of Pennsylvania

Hui Wu
University of Pennsylvania

See next page for additional authors

Copyright American Physical Society. Reprinted from *Physical Review Letters*, Volume 98, Article 107601, 4 pages.
Publisher URL: http://dx.doi.org/10.1103/PhysRevLett.98.107601

Structure and Polarization in the High T_c Ferroelectric $Bi(Zn,Ti)O_3$-$PbTiO_3$ Solid Solutions

Abstract
Theoretical *ab initio* and experimental methods are used to investigate the $[Bi(Zn_{1/2}Ti_{1/2})O_3]x\,[PbTiO_3]1\text{-}x$ solid solution. We find that hybridization between Zn 4*s* and 4*p* and O 2p orbitals allows the formation of short, covalent Zn-O bonds, enabling favorable coupling between *A*-site and *B*-site displacements. This leads to unusually large polarization, strong tetragonality, and an elevated ferroelectric to paraelectric phase transition temperature.

Publisher URL: http://dx.doi.org/10.1103/PhysRevLett.98.107601

Author(s)
Ilya Grinberg, Matthew R. Suchomel, Wotjek Dmowski, Sara E. Mason, Hui Wu, Peter K. Davies, and Andrew M. Rappe

Structure and Polarization in the High T_c Ferroelectric Bi(Zn, Ti)O_3-$PbTiO_3$ Solid Solutions

Ilya Grinberg,[1] Matthew R. Suchomel,[2] Wojtek Dmowski,[3] Sara E. Mason,[1] Hui Wu,[2]
Peter K. Davies,[2] and Andrew M. Rappe[1]

[1]*The Makineni Theoretical Laboratories, Department of Chemistry, University of Pennsylvania, Philadelphia, Pennsylvania 19104-6323, USA*

[2]*Department of Materials Science and Engineering, University of Pennsylvania, Philadelphia, Pennsylvania 19104-6272, USA*

[3]*Department of Materials Science and Engineering, University of Tennessee, Knoxville, Tennessee 37996, USA*

(Received 31 March 2006; published 5 March 2007)

Theoretical *ab initio* and experimental methods are used to investigate the $[Bi(Zn_{1/2}Ti_{1/2})O_3]_x$ $[PbTiO_3]_{1-x}$ solid solution. We find that hybridization between Zn 4*s* and 4*p* and O 2*p* orbitals allows the formation of short, covalent Zn-O bonds, enabling favorable coupling between *A*-site and *B*-site displacements. This leads to unusually large polarization, strong tetragonality, and an elevated ferroelectric to paraelectric phase transition temperature.

DOI: 10.1103/PhysRevLett.98.107601 PACS numbers: 77.80.Dj, 61.66.Fn, 71.15.Mb, 77.84.Dy

Because of their importance in ferroelectric and piezoelectric applications and their fascinating physical properties, perovskite solid solutions have been an area of active research [1–5]. In particular, Bi-based ferroelectrics are under intense investigation, as they exhibit extremely large polarization [6,7] and in some cases multiferroic behavior [8,9]. In addition, the better environmental characteristics of Bi versus Pb make Bi-based ferroelectrics of great technological interest. It has been known for some time that the most favorable piezoelectric properties are found at the morphotropic phase boundary (MPB) between the rhombohedral and tetragonal ferroelectric phases. The Pb(Zr, Ti)O_3 solid solution is the current material of choice for piezoelectric applications, due to its high piezoelectric performance at the MPB composition.

To create Bi-based analogs of the current Pb(Zr, Ti)O_3 piezoelectric materials, a mixture of tetragonal and rhombohedral end members is necessary. While many Bi-based materials exhibit rhombohedral or octahedrally tilted structures analogous to $PbZrO_3$, tetragonal Bi-based materials analogous to $PbTiO_3$ are quite rare, due to the small size of the Bi ion. Large (100) oriented polarization is also favorable for applications in ferroelectric nonvolatile memory devices. Recently, it was shown that large tetragonality ($c/a \approx 1.11$) and high T_c ($\approx$1000 K) can be obtained in the $[Bi(Zn_{1/2}Ti_{1/2})O_3]_x[PbTiO_3]_{1-x}$ (BZT-PT) solid solution [6]. This makes BZT-PT a promising candidate material for use in next-generation piezoelectric and nonvolatile memory applications. In particular, the rate of increase in both properties as BZT replaces PT is the largest known for any PT-based perovskite solid solution. Currently, the extremely strong tetragonality enhancement in BZT-PT is only matched by tetragonal materials such as $PbVO_3$ [10,11] and $BiCoO_3$ [7,9] where partially filled *d* states are present, making these materials poor candidates for technological applications due to their low resistivity. In contrast, BZT and related compounds are d^0 materials, which gives them excellent resistivity, making them true ferroelectrics with polarization switchable by electric field. We note that the Bi(Mg, Ti)O_3-PT (BMT-PT) solid solution, which does not exhibit anomalous c/a increase [12], differs from the BZT-PT system only by the isovalent *B*-site cation replacement of Mg for Zn. Thus, the rare combination of high tetragonality and d^0 electronic structure found in BZT-PT is due to the presence of Zn ions. In this Letter, we combine theoretical calculations with new experimental data to reveal the origins of anomalous behavior in the BZT-PT system.

To determine the local, Å-scale structure in the BZT-PT system, we performed density functional theory [13] (DFT) calculations using $2 \times 2 \times 2$ 40-atom supercells with periodic boundary conditions at experimental volume [6]. Technical details are the same as in previous work [14]. We use five and seven different cation arrangements with minimal oxygen over- and underbonding [14–16] to study $x = 0.25$ and $x = 0.5$ compositions, respectively. Polarization magnitudes were calculated using the Berry-phase approach [17].

Results of theoretical calculations were compared with experimental structural information obtained from neutron powder diffraction (NPD) of selected compositions in the $[BZT]_x[PT]_{1-x}$ system. The neutron powder diffraction data were collected under ambient conditions over the range 3°–165° 2θ using the BT-1 32 detector neutron powder diffractometer at the NIST Center for Neutron Research. Full details of the experimental data and the Rietveld structural refinements can be found in Ref. [18]. Additional structural information was extracted from the neutron-scattering data collected on the NPDF instrument at the Los Alamos National Science Center (LANSCE) by pair distribution function (PDF) analysis techniques; details of this experimental procedure have been described previously [19].

The spectra obtained from NPD exhibited some unusual features. This necessitated a more complex Rietveld refinement procedure to accurately extract structural data from the NPD spectra. In Fig. 1, we present the 40°–60° 2θ neutron diffraction data for the $x = 0.35$ composition [20].

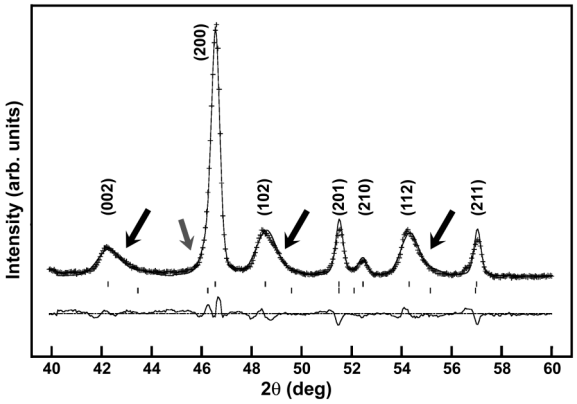

FIG. 1. Experimental and refined neutron diffraction data plotted in the 40°–60° 2θ range for the $x = 0.35$ composition. Crosses indicate experimental data, two-phase fit shown by solid line and fit difference is marked at bottom. Black arrows point to asymmetric broadening of l-containing peaks, while the gray arrow highlights the more subtle h, k peak broadening.

Arrows point out clearly visible asymmetric peak broadening on the high 2θ angle side of the $l \neq 0$ peak reflections [(001), (102), etc.]. Although less marked, asymmetric broadening is also present on the low 2θ angle side of h/k-containing peak reflections. It is well known that peak broadening in diffraction experiments can have various causes, including small crystalline particle size or an internally stressed sample. However, both of these possible origins would result in symmetrical peak broadening. In contrast, the broadening observed in the NPD presented here, and in x-ray diffraction data of the $[BZT]_x[PT]_{1-x}$ system [6], is quite strongly asymmetrical.

A two-phase Rietveld refinement is necessary to achieve a high-quality fit of the NPD data and to extract reliable structural parameters. Here, we assume that two structurally similar phases are present in the material for the $x = 0.20$ and $x = 0.35$ compositions. We note that a single phase Rietveld refinement would not reproduce the asymmetric broadening and would result in a low-quality fit [21]. Full details of this refinement are available online.

We find excellent agreement (Fig. 1) for a model where the majority or bulk phase (90% of the material) is a perovskite with a large c/a ratio ($c/a = 1.095$ for $x = 0.35$), and a minority phase is a perovskite of smaller c/a ($c/a = 1.060$ for $x = 0.35$). Such a model was previously used to model asymmetric broadening in the parent $PbTiO_3$ material, where the differences in the lattice parameters between the two phases were assigned to the local suppression of polarization and tetragonality next to a domain wall in unpoled crystalline samples [21]. In materials which undergo ferroelastic phase transitions, large elastic strain conditions make sharp changes in polarization caused by the presence of the microstructure (e.g., surfaces and domain and grain boundaries) energetically unfavorable. However, the energy cost can be minimized by the creation of a narrow region of locally suppressed polarization and tetragonality. This leads to local distortions in the a and c lattice parameters.

In addition to the intrinsic reflections resulting from the bulk material, the l-containing peak reflections of a sample with this structure will also exhibit a broad asymmetrical tail on the high 2θ angle side of the fundamental peak. This broadening effect is due to reflection contributions from reduced c axes in the microstructural boundary region. The increase in the a and b lattice parameters in the near-boundary region, driven by conservation of unit cell volume and rotation of polarization [22], will give additional asymmetrical tails on the low 2θ angle side of the fundamental h/k-containing peak reflections. It is possible that local suppression of polarization and tetragonality at microstructural boundaries causes the asymmetric broadening observed in our BZT-PT samples as well.

Irrespective of the physical origins of the asymmetric broadening, the two-phase model refinement gives us high-resolution information on the structure of the majority intrinsic phase. A summary of structural data obtained from both DFT calculations and refined NPD data are shown in Table I. This compares the measured and predicted (100) cation displacements for several compositions in the $[BZT]_x[PT]_{1-x}$ system and reveals very good agreement between the theoretically and experimentally determined values [23].

While displacements determined by refinement of the NPD data show only average A and B site behavior, in the DFT calculations it is possible to distinguish between the chemically distinct cations occupying each cation site in the tetragonal perovskite structure. A closer examination of the different behavior of the cations in the $[BZT]_x[PT]_{1-x}$ system helps us understand its anomalous behavior.

We find that Zn displacements are very large, reaching 0.5 Å in the $x = 0.50$ composition. The combination of the low valence of Zn and the long, ≈2.6 Å Zn-O distances created by the large displacements eliminates the bond between Zn and one of its six O neighbors, transforming the Zn-O_6 cages into Zn-O_5 complexes. The unusually

TABLE I. $[BZT]_x[PT]_{1-x}$ structural data obtained from DFT relaxed coordinates for $x = 0.25$ and $x = 0.5$ compositions and from Rietveld refinement of experimental neutron diffraction data (NPD) for $x = 0.20$ and $x = 0.35$ compositions. Cation displacements are from the center of the oxygen cage in Å. Pb cation displacement scatter rotation away from the (100) direction (θ_{Pb}) in degrees. For experimentally investigated compositions, only average characteristics of A- and B-sites are available. Data are for the intrinsic high c/a structure. P is given in C/m^2

x	Data	Pb Disp.	Bi Disp.	Avg. A Disp.	Zn Disp.	Ti Disp.	Avg. B Disp.	θ_{Pb}	P
0	DFT	0.44	···	0.44	···	0.28	0.28	0	0.88
0.20	NPD	···	···	0.56	···	···	0.23	···	···
0.25	DFT	0.49	0.82	0.59	0.38	0.32	0.33	13	1.03
0.35	NPD	···	···	0.60	···	···	0.29	···	···
0.50	DFT	0.56	0.90	0.73	0.50	0.34	0.38	18	1.27

large Zn distortions are due to the hybridization of 4s and 4p orbitals of Zn with 2p orbitals of O atoms. Local atom-projected density of states (LDOS) [Fig. 2(a)] shows that Zn 4s and 4p orbitals are partially filled in $[BZT]_x[PT]_{1-x}$, due to covalent bonding with oxygen 2p states. This is similar to the LDOS of covalently bonded Ti ions in $PbTiO_3$ (where the hybridization is between Ti 3d and O 2p) [1], and is in stark contrast to the highly ionic bonding of Mg ions in BMT-PT [24]. In comparison with Zn, Ti displacements in the $[BZT]_x[PT]_{1-x}$ system hardly change with alloying x. From $x = 0.25$ to $x = 0.50$, the calculated Ti cation displacement only increases from 0.32 to 0.34 Å. Even for $x = 0.50$ composition, the Ti-O_6 cage is largely preserved, with average bond order ≈ 0.25 [25] for the long Ti-O bond distances. The large Ti displacements are enabled by the Zn off-centering, due to coupling between B-cation displacements [14,26].

Both our experimental and theoretical data (Table I) show that large Bi and Pb distortions are present in the BZT-PT solid solutions. The typical Bi distortion magnitudes are about 0.80 and 0.90 Å for $x = 0.25$ and $x = 0.50$, respectively. The magnitudes of Bi displacements found in this study are much larger than the 0.5 Å distortion found for Bi in $BiFeO_3$ [27]. Addition of BZT also induces a 10%–20% increase in Pb displacement magnitudes. Analysis of Bi-O_{12} and Pb-O_{12} cages reveals a crucial difference between the bonding behavior of the two A-site cations. Bi displacements create three or four very short ($\approx$2.1–2.2 Å) and strong (bond order $\approx$0.6–0.8) Bi-O bonds. This motif was also found by a recent x-ray absorption fine structure study of the (K, Bi)TiO_3-(Na, Bi)TiO_3 solid solution [28]. Bond valence analysis [25] shows that typically 70%–90% of the Bi-O bonding is with these three or four closest O atoms, while the other O atoms are located far enough from Bi to make their contribution to the bonding negligible. Essentially, the large Bi displacements create a Bi-O_3 or Bi-O_4 complex out of the Bi-O_{12} cage. In contrast, although the Pb atoms also make three or four short Pb-O bonds, the larger ionic size of Pb and its smaller displacement magnitude mean that the differences among Pb-O bond lengths are smaller. The shortest three or four Pb-O bonds typically account for only 40%–60% of the total Pb-O bond order. Thus, the difference in ionic sizes of Pb^{2+} (1.49 Å) and Bi^{3+} (1.36 Å) gives rise to different A-O bonding motifs.

To confirm that DFT calculations accurately reproduce structural motifs, we performed neutron-scattering experiments. In agreement with DFT results, we find that substitution of BZT for PT leads to a broad PDF, indicative of a material with strong local distortions from the overall structure. We find that PDFs show only slight variations among the various supercells used in the DFT calculations. Comparison of the neutron-scattering PDF for $x = 0.20$ and the relaxed DFT PDF for $x = 0.25$ shows excellent agreement between theory and experiment [Fig. 2(b)]. The shoulder at 2.2 Å in the experimental PDF is due to the short Bi-O distances created by the large Bi displacements. In the higher-resolution DFT PDF, another shoulder is apparent at 2.5 Å, consistent with the off-center displacement of Pb ions [16,29].

The local structure distortions determined by our DFT calculations manifest themselves in the observed structural and dielectric properties of the BZT-PT solid solution. The increase in the c axis lattice parameter is driven by the large magnitude of Bi distortions. This is because the energy lowering obtained by A-site displacement couples strongly to the strain in the material [1,30–32]. An increase of c parameter also alleviates large direct and oxygen-mediated A-B repulsions created by the large Bi displacements [3,14].

In contrast to other solid solutions, the B sites of BZT-PT are completely occupied by ferroelectrically active (Zn and Ti) ions that can form short, covalent bonds with oxygen. For these cations, the large B-site displacement necessitated by large Bi displacements and A-B displacement coupling [3,14,33] are favorable. Consequently, there is no energetic penalty for making large off-center displacements necessitated by a combination of large Bi-cation displacements and oxygen bond order conservation. This stabilizes the tetragonal perovskite phase [33]. While ad-

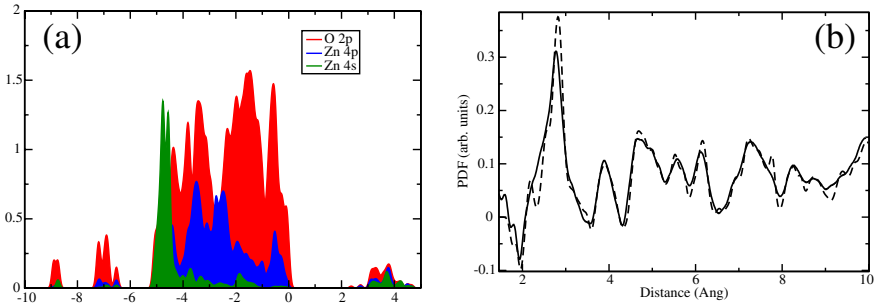

FIG. 2 (color online). (a) Local density of states for Zn and O in $[BZT]_x[PT]_{1-x}$. A cutoff radius of 2 Å was used to perform the projection on atomic orbitals of Zn and O. Strong hybridization is present between Zn 4s and 4p and O 2p orbitals. This allows formation of short covalent Zn-O bonds and favors large Zn off-centering. (b) $[BZT]_x[PT]_{1-x}$ pair distribution functions (PDF) obtained by neutron-scattering for $x = 0.20$ (solid) and computed from relaxed DFT structures for $x = 0.25$ (dashed). The experimental and theoretical data show excellent agreement.

dition of BZT increases the c axis parameter, the a axis parameter is virtually unchanged with composition. This is most likely due to the fact that Ti-O octahedra are rather stiff, and there is a significant energy cost for compressing Ti-O bonds along the short (010) and (001) directions [30]. The decrease in the a axis parameter is also disfavored by the large ionic size of Zn^{+2}.

The local structural distortions (reported above) for BZT-PT also help rationalize the increase in transition temperature. Reported dielectric permittivity for the $[BZT]_x[PT]_{1-x}$ system [6] shows that increased BZT content causes a nonlinear rise in the temperature of the dielectric maximum ($T_{\epsilon,\max}$). The trend in $T_{\epsilon,\max}$ can be understood by considering the changes of polarization magnitude with BZT content in conjunction with the previously established relationship that $T_{\epsilon,\max}$ is proportional to P^2 for PT-based solutions [14,19,34]. Using Berry-phase calculated P values for pure PT ($x = 0.0$), $x = 0.25$ and $x = 0.5$ compositions, we see that the increase in $T_{\epsilon,\max}$ correlates with the enhancement of P, with extremely high P values of 1.03 ± 0.05 C/m^2 and 1.27 ± 0.05 C/m^2 for the $x = 0.25$ and $x = 0.50$ compositions, respectively (Table I). This is due to the large cation displacements present in these compositions.

In conclusion, we have examined the enhanced tetragonality BZT-PT solid solution with a combination of experimental and first-principles methods. Favorable coupling between A-site and B-site cation displacements gives rise to large polarization magnitudes. The behavior of Zn and its origins elucidated here suggest that Zn substitution for Mg could be a useful tool for a variety of ferroelectrics as well as for other types of materials, where the ability of Zn to form covalent bonds will give radically different behavior than that of the Mg analog.

This research was supported by the Office of Naval Research, under Grants No. N-000014-00-1-0372 and No. N00014-01-1-0860 and through the Center for Piezoelectrics by Design. We also acknowledge the support of the National Science Foundation, through the MRSEC program, Grant No. DMR05-20020, the use of NPDF spectrometer at LANSCE, Los Alamos National Lab., and the use of BTI diffractometer at NIST Center for Neutron Research. Computational support was provided by the Center for Piezoelectrics by Design, the DoD HPCMO, DURIP and by the NSF CRIF program, Grant No. CHE-0131132.

[1] R. E. Cohen, Nature (London) **358**, 136 (1992).
[2] L. Bellaiche, A. Garcia, and D. Vanderbilt, Phys. Rev. Lett. **84**, 5427 (2000).
[3] I. Grinberg, V. R. Cooper, and A. M. Rappe, Nature (London) **419**, 909 (2002).
[4] Y. Saito *et al.*, Nature (London) **432**, 84 (2004).
[5] R. E. Eitel *et al.*, Jpn. J. Appl. Phys. **40**, 5999 (2001).
[6] M. R. Suchomel and P. K. Davies, Appl. Phys. Lett. **86**, 262905 (2005).
[7] Y. Uratani, T. Shishidou, F. Ishii, and T. Oguchi, Jpn. J. Appl. Phys. **44**, 7130 (2005).
[8] J. Wang *et al.*, Science **299**, 1719 (2003).
[9] A. A. Belik *et al.*, Chem. Mater. **18**, 798 (2006).
[10] R. V. Shpanchenko *et al.*, Chem. Mater. **17**, 269 (2005).
[11] D. J. Singh, Phys. Rev. B **73**, 094102 (2006).
[12] M. R. Suchomel and P. K. Davies, J. Appl. Phys. **96**, 4405 (2004).
[13] J. P. Perdew and A. Zunger, Phys. Rev. B **23**, 5048 (1981).
[14] I. Grinberg and A. M. Rappe, Phys. Rev. B **70**, 220101 (2004).
[15] B. P. Burton and E. Cockayne, Phys. Rev. B **60**, R12542 (1999).
[16] I. Grinberg, V. R. Cooper, and A. M. Rappe, Phys. Rev. B **69**, 144118 (2004).
[17] R. D. King-Smith and D. Vanderbilt, Phys. Rev. B **47**, 1651 (1993).
[18] See EPAPS Document No. E-PRLTAO-98-018707 for supporting information. For more information on EPAPS, see http://www.aip.org/pubservs/epaps.html.
[19] P. Juhas *et al.*, Phys. Rev. B **69**, 214101 (2004).
[20] Diffraction data for the full 2θ range and a complete summary of Rietveld refinement results can be found in Ref. [18].
[21] H. Boysen, Z. Kristallogr. **220**, 726 (2005).
[22] B. Meyer and D. Vanderbilt, Phys. Rev. B **65**, 104111 (2002).
[23] Unsurprisingly, the ionic displacements found by the low c/a phase refinements ($\approx$0.5 Å for the A-site displacement and $\approx$ 0.25 Å for the B-site displacement for $x =$ 0.20 and $x = 0.35$) are quite different from DFT results, since the strain gradients present in the proposed microstructure were not included in the DFT calculations.
[24] Calculated LDOS for BMT-PT shows that in contrast to Zn, the Mg 3s states are completely empty.
[25] I. D. Brown, in *Structure and Bonding in Crystals II*, edited by M. O'Keefe and A. Navrotsky (Academic Press, New York, 1981), pp. 1–30.
[26] P. Ghosez *et al.*, Phys. Rev. B **60**, 836 (1999).
[27] J. B. Neaton *et al.*, Phys. Rev. B **71**, 014113 (2005).
[28] V. A. Shuvaeva *et al.*, Phys. Rev. B **71**, 174114 (2005).
[29] T. Egami, W. Dmowski, M. Akbas, and P. K. Davies, in *First-Principles Calculations for Ferroelectrics*, edited by R. E. Cohen (American Institute of Physics, Melville, New York, 1998), pp. 1–10.
[30] S. V. Halilov, M. Fornari, and D. J. Singh, Phys. Rev. B **69**, 174107 (2004).
[31] S. V. Halilov, M. Fornari, and D. J. Singh, Appl. Phys. Lett. **81**, 3443 (2002).
[32] M. Ghita *et al.*, Phys. Rev. B **72**, 054114 (2005).
[33] I. Grinberg *et al.*, J. Appl. Phys. **98**, 094111 (2005).
[34] S. C. Abrahams, S. K. Kurtz, and P. B. Jamieson, Phys. Rev. **172**, 551 (1968).